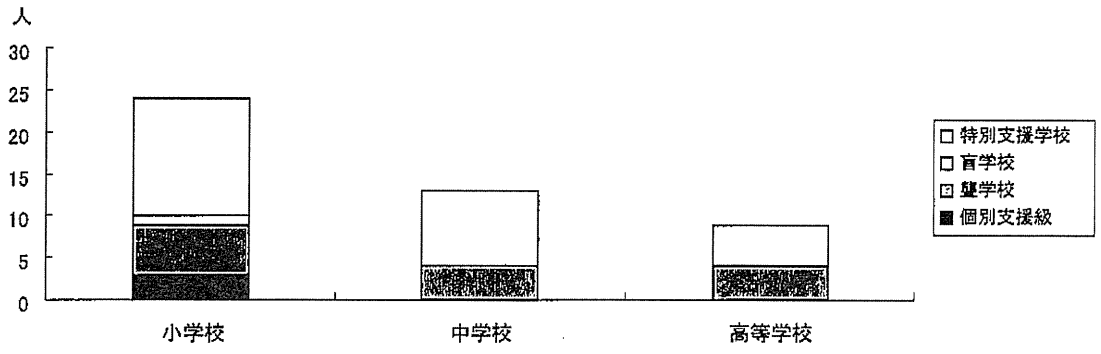

図3 就学状況

視覚・聴覚障害を合併しているため精神発達の正確な評価は困難であった．知能検査が施行された症例は12例であり，IQ40以下が7例，IQ40～50が4例であった．動作性IQのみを測定された1例では，動作性IQ 100と正常であった．境界～軽度の精神遅滞と思われる症例の中には，高校生でワープロ検定取得をした症例や，高校卒業後に専門学校に進学している症例が存在した．また身辺自立が達成できている症例は5例であった．

コミュニケーション能力は，手話もしくは手話＋音声によって会話が成立する症例が10例，家族や学校の先生などの身近な人と，ジェスチャーやサイン，絵や写真を用いたカードなどで簡単なやりとりが可能な症例が9例であった(図2参照)．コミュニケーション手段を獲得することにより，社会性の獲得が急速に進む傾向がみられた．

知的障害が軽度～中等度でコミュニケーションが可能な症例の行動の傾向としては，コミュニケーション手段が確立する幼児期～学童期において，陽気で人懐っこい性格の傾向がある一方で，せわしなく，落ち着きがないという行動が目立った．身辺自立が可能で，境界～軽度の知的障害と思われる症例のうち2例には夜尿を認め，知的障害が重度～中等度のうち3例では，自傷行為を認めた．

⑯その他の合併症

反回神経麻痺6例，左片側内頸動脈部分低形成1例，重度の低血糖，ショックによる低酸素性虚血性脳症1例の合併を認めた．

4．就学・就労状況

就学状況を図3に示す．小学校就学（24例）では，特別支援学校が14例と約半数を占め，聾学校6例，特別支援学級3例，盲学校1例であった．中学校（13例）では，特別支援学校9例，聾学校4例，高等学校（9例）では特別支援学校5例，聾学校4例であった．高校卒業後に専門学校に進学している症例が1例，作業所で就労している症例が1例であった．

考　察

診断確定告知年齢は新生児期から20代と幅広く，3歳までに約2/3の症例が診断告知されていた．就学以降に診断された症例は8例であり，診断確定が遅れる症例も目立った．診断が遅れる理由としては，新生児期～乳児期は合併症管理が中心となり，合併症が多岐にわたり複数の診療科がかかわるため，総合的に診察し診断する機会を逃していることが考えられる．しかし，近年では医療サイドの疾患の認知度の向上により，診断が早まっている傾向もみられた．

合併症の頻度に関しては，先天性心奇形，コロボーマ，外耳奇形・難聴，性腺機能低下（外性器異常も含む）はこれまで報告[9)~12)]されている頻度とほぼ同程度であった．一方で，後鼻孔閉鎖が30%，食道閉鎖が1例とこれまでの報告より頻度が少なく，口唇・口蓋裂は38%と頻度が高い結果であった．

CHSは喉頭軟化症や摂食嚥下障害の重症度によっては，長期にわたり濃厚な医療管理を必要とする症例が少なくない．今回の結果でも，喉頭軟化症は26例中23例に合併し頻度は高く，このうち1か月以上の長期呼吸管理を要した重症例は7例であった．7例中，気管切開を施行したのは3例で，このうち2例は症状が改善し5歳，9歳の時に気管切開孔の閉鎖を行っていた．また軽度～中等度の症例でも，呼吸器感染時には入院を要し，乳児期には入院治療が頻回となる傾向があった．摂食嚥下障害も全例に認め，胃食道逆流は約半数に合併し，約1/4の症例は噴門形成術や胃瘻造設術の外科的治療を要していた．また栄養摂取については，経口摂取が進まず，長期にわたって経腸栄養の併用を要する症例が多く，経口のみで栄養摂取が可能な症例も，口腔過敏や嚥下障害のために年長になっても液体やペースト形態の食物や栄養剤しか摂取できないという問題を抱えていた．このように，CHSでは呼吸・気道の問題，摂食・嚥下の問題はほぼ全例に認め，長期にわたり医療管理を要する症例が多く，家族の負担も

大きい．早期に診断を確定することによって，これらの問題が起こる可能性と，長期的な見通しについて家族に説明し，支援をしていくことが重要と思われる．また，気管切開や胃瘻などの医療管理を要する症例の中には，長期的にみると症状の改善が得られ，気管孔閉鎖，胃瘻閉鎖が可能となる例が少なくないという点も，医療サイドや家族にとって，貴重な情報と思われる．

三半規管や斜台の低形成，嗅球・嗅溝の低形成，無形成はCHSに多くみられる所見とされている[17)19)]．今回も検査を施行した全例でこれらの所見を認めており，内耳，側頭骨および嗅球・嗅溝の画像評価が，診断には有用と思われた．

特異な経過をとった症例として，症例18は1歳6か月時に感染を契機に著しい低血糖，ショックとなり，その結果，低酸素性虚血性脳症を呈し，後遺症として重度精神運動発達遅滞，痙性麻痺，てんかんを認めている．低血糖とショックの原因として，副腎不全が疑われたが，証明はできていない．Jamesらは，新生児期に低ナトリウム血症，低血糖を呈し副腎不全を認めた症例を報告しており[22)]，CHSの患者で発汗，冷感，意識障害を認めた場合は，低血糖の可能性を念頭に置いて，速やかにグルコースの輸液を開始するべきであると提唱している．

運動発達に関しては，乳児期～小児期の粗大運動の遅れは筋緊張低下や視力障害，平衡感覚の異常などからCHSのほぼ全例に認めるとされている．今回の結果では，26例中21例が2～8歳までに独歩を獲得し，独歩獲得年齢の平均は4.4歳であり，運動発達の遅れは明かであった．股関節臼蓋形成不全や低酸素性虚血性脳症後遺症のため独歩が獲得できない症例以外に，整形学的，神経学的な理由がないにもかかわらず，学童期になっても独歩不可能の症例を2例認め，運動発達遅滞が重度の症例も存在していた．

精神発達については，視覚障害，聴覚障害の合併が多いため，十分な評価が困難であり判断には注意を要する．また知的障害はCHSに必ず認める所見ではないと考えられている．今回，知能検査が施行された12例のIQ/DQは<20～48と，重度～中等度の精神遅滞と判定されており，聴覚障害のため言語性IQ/DQが低い傾向にあった．しかし，症例9は，動作性のみの評価でIQ100と正常であり，症例6は高校生でワープロ3級取得していた．正確な知能の評価は難しいものの，これらの症例の精神発達は境界領域～軽度であると考えられた．また10例が手話（＋音声）を，9例は簡単なジェスチャー・サイン，カードなどを用いて，コミュニケーションが可能であり，身辺自立を達成できている症例もいた．特に手話やジェスチャー・サインなどの手段を獲得できない年少児においては，絵や写真を用いた視覚的に認識できるカードが有効であった．

CHSでは，中等度～重度の行動の異常がみられることが知られている[14)～16)]．その行動特性は視覚障害や聴覚障害の有無や重症度によって異なるとされ，具体的には，強迫性障害，注意欠陥障害，Tourette症候群，自閉症などに分類され，時には興奮しすぎて，自分の感情をコントロールするのが困難となるという場合もあるとされる．しかし彼らにとっては，これらの行動特性は，社会性を獲得するためのコミュニケーション手段そのものであると考えられている．知的障害が軽度～中等度で視覚，聴覚の両者の障害をもつ症例の行動としては，陽気で人懐っこい性格の傾向がある一方で，忙しなく，落ち着きがないという行動が目立った．これらの特徴がCHS特有の行動特性なのか，視覚障害や聴覚障害を含めたさまざまな合併症によって二次的に生じている行動特性なのかを明らかにするのは難しい．しかし，相手と関わることのできる喜びや興奮が過度となりすぎること，また，自分の思っていることがなかなか相手に伝わらないというフラストレーションや焦りなどが，忙しなさや落ち着きのなさという行動特性に影響している可能性は考えられる．知的障害が中等度～重度な症例の中には，コミュニケーション能力が低いために，フラストレーションが溜って，自傷行為に結びついているのではないかと考えられ，また知的障害が境界～軽度の2例で認められた夜尿も心因性要因が関連している可能性が考えられる．

CHSは，視覚障害，聴覚障害に加えて，さまざまな合併症を抱えている．特に濃厚な医療管理を必要としている症例においては重症感が伴い，知的障害が重度なのではないかと誤解される場合もある．しかし，今回行ったコミュニケーション能力についての検討や我々の臨床的な経験から，CHSの中には実際のパフォーマンスに比べて理解力が高いと思われる症例が存在することが示唆された．このことより，早期に視覚障害，聴覚障害に対して介入し，療育を行うことによって，彼らの潜在的な発達の可能性を充分に引き出し，コミュニケーション能力を育てることが，精神行動面の安定化，そして社会性の獲得につながると考えられる．

CHSの長期的なフォローアップには，多岐にわたる合併症や成長発達の特徴，行動特性などの自然歴をふまえたうえで，医療，療育，教育の専門家が正しく疾患を理解し，個々の患者にあわせて適切な管理を行い生活の質を向上させることが，患者と家族にとって最も重要と考える．

本論文の要旨は第113回日本小児学会学術集会（2010年，岩手）において発表した．

本研究の一部は厚生労働科学研究費補助金（難治性疾患克服研究事業）によって行われたものである．

謝辞 *CHD7*遺伝子変異解析を行っていただいた慶応義塾大学医学部小児科の小崎健次郎先生に深謝いたします．

日本小児科学会の定める利益相反に関する事項はありません．

文 献

1) Pagon RA, Graham JM Jr, Zonana J, et al. Coloboma, congenital heart disease, and choanal atresia with multiple anomalies : CHARGE association. J Pediat 1981 ; 99 : 223—227.
2) Blake KD, Davenport SLH, Hall BD, et al. CHARGE association : an update and review for the primary pediatrician. Clin Pediatr 1998 ; 37 : 159—173.
3) Tellier AL, Cormier-Daire V, Abadie V, et al. CHARGE syndrome : report of 47 cases and review. Am J Med Genet 1998 ; 76 : 402—409.
4) Wheeler PG, Quigley CA, Sadeghi-Nejad A, et al. Hypogonadism and CHARGE association. J Med Genet 2000 ; 94 : 228—231.
5) Vissers LE, van Ravenswaaij CM, Admiraal R, et al. Mutations in a new member of the chromodomain gene family cause CHARGE syndrome. Nat Genet 2004 ; 36 : 955—957.
6) Verloes A. Updated diagnostic criteria for CHARGE syndrome : A proposal. Am J Med Genet A 2005 ; 133 A : 306—308.
7) Blake KD, Hartshorne TS, Lawand C, et al. Cranial nerve manifestations in CHARGE syndrome. Am J Med Genet A 2008 ; 146A : 585—592.
8) Issekutz KA, Smith IM, Prasad C, et al. An epidemiological analysis of CHARGE syndrome : preliminary results from a Canadian study. Am J Med Genet A 2005 ; 133 : 309—317.
9) Zentner GE, Layman WS, et al. Molecular and phenotypic aspects of CHD 7 mutation in CHARGE syndrome. Am J Med Genet A 2010 ; 152A : 674—686.
10) Lalani SR, Safiullah AM, Fernbach SD, et al. Spectrum of CHD7 mutations in 110 individuals with CHARGE syndrome and genotype-phenotype correlation. Am J Hum Genet 2006 ; 78 : 303—314.
11) Jongmans M, Admiraa R, van der Donk K, et al. CHARGE syndrome : the phenotypic spectrum of mutations in the CHD7 gene. J Med Genet 2005 ; 43 : 306—314.
12) Aramaki M, Udaka T, Kosaki R, et al. Phenotypic spectrum of CHARGE syndrome with CHD7 mutations. J Pediatr 2006 ; 148 : 410—414.
13) Dobbelsteyn C, Peacocke SD, Blake K, et al. Feeding difficulties in children with CHARGE syndrome : prevalence, risk factors, and prognosis. Dysphagia 2008 ; 23 : 127—135.
14) Hartshorne TS, Hefner M, Davenport S. Behavior in CHARGE syndrome : introduction to the special topic. Am J Med Genet A 2005 ; 133 : 228—231.
15) Hartshorne TS, Heussler HS, Dailor AN, et al. Sleep disturbances in CHARGE syndrome : types and relationships with behavior and caregiver well-being. Dev Med Child Neurol 2009 ; 51 : 143—150.
16) Hartshorne TS, Grialou TL, Parker KR. Autistic-like behavior in CHARGE syndrome. Am J Med Genet A 2005 ; 133A : 257—261.
17) Fujita K, Aida N, Asakura Y, et al. Abnormal basiocciput development in CHARGE syndrome. AJNR Am J Neuroradiol 2009 ; 30 : 629—634.
18) Wheeler PG, Quigley CA, Sadeghi-Nejad A, et al. Hypogonadism and CHARGE association. Am J Med Genet 2000 ; 94 : 228—231.
19) Asakura Y, Toyota Y, Muroya K, et al. Endocrine and radiological studies in patients with molecularly confirmed CHARGE syndrome. J Clin Endocrinol Metab 2008 ; 93 : 920—924.
20) 川目 裕. 主要な先天異常症候群のメディカル・マネージメント. CHARGE症候群 2005 ; 37 : 1333—1338.
21) Cassidy SB, Allanson JE. Management of Genetic Syndromes. 3rd ed. Wiley-Blackwell, 2010.
22) James PA, Aftimos S, Hofman P. CHARGE association and secondary hypoadrenalism. Am J Med Genet A 2003 ; 117A : 177—180.

Clinical Features in 26 Patients with CHARGE Syndrome

Aki Ishikawa[1], Keisuke Enomoto[1], Noritaka Furuya[1], Kouji Muroya[2], Yumi Asakura[2], Masanori Adachi[2] and Kenji Kurosawa[1]
[1]Division of Medical Genetics, Kanagawa Children's Medical Center
[2]Division of Endocrinology & Metabolism, Kanagawa Children's Medical Center

CHARGE syndrome is a congenital malformation syndrome characterized by a nonrandom occurrence of anomalies including coloboma, heart defects, choanal atresia, retarded growth and development, genital abnormalities, and ear anomalies/deafness. To elucidate the natural history and medical managements of the syndrome, we reviewed the clinical features of 26 patients with CHARGE syndrome who received follow-up care at our Children's Medical Center. The ages at diagnosis varied widely from neonates to adolescents. The most common clinical findings, including external ear malformations, hearing loss, and developmental delays, were recognized in all patients, followed by growth retardation (92%), coloboma (77%), congenital heart defects (84%), and genital hypoplasia/hypogonadotropic hypogonadism (84%). Eight patients (30%) had choanal atresia as a cardinal feature of CHARGE syndrome, but esophageal atresia, which is one of the major complications, was found in only one case. An MRI survey on the semicircular ducts and olfactory bulb provided useful information for clinical diagnosis of the syndrome. Because of cognitive retardation associated with visual disturbance and deafness, evaluation of the patients' potentials for development is difficult. However, approximately 80% of patients were able to communicate by manualism, gestures, and signs, and these results suggested a discrepancy between congenital potential ability and their real performance. Patients with CHARGE syndrome frequently had behavioral difficulties, attention deficits, and hyperactivity. These characteristic types of behavior may be partially related to problems of arousal, self-regulation, and frustration. Ophthalmologic evaluation and auditory examination should be performed as early as possible in CHARGE syndrome patients. Our study results will be useful for diagnosis, medical managements of complications, and rehabilitations of CHARGE syndrome patients. We believe that a better knowledge of the underlying syndrome leads to better familial understanding and acceptance, and could provide insight into the prognosis.

Familial Cancer
DOI 10.1007/s10689-013-9623-1

ORIGINAL ARTICLE

Frameshift mutation in the *PTCH2* gene can cause nevoid basal cell carcinoma syndrome

Katsunori Fujii · Hirofumi Ohashi · Maiko Suzuki · Hiromi Hatsuse · Tadashi Shiohama · Hideki Uchikawa · Toshiyuki Miyashita

Abstract Nevoid basal cell carcinoma syndrome (NBCCS) is an autosomal dominant disorder characterized by developmental defects and tumorigenesis. The gene responsible for NBCCS is *PTCH1*, encoding a receptor for the secreted protein, sonic hedgehog. Recently, a Chinese family with NBCCS carrying a missense mutation in *PTCH2*, a close homolog of *PTCH1*, was reported. However, the pathological significance of missense mutations should be discussed cautiously. Here, we report a 13-year-old girl diagnosed with NBCCS based on multiple keratocystic odontogenic tumors and rib anomalies carrying a frameshift mutation in the *PTCH2* gene (c.1172_1173delCT). Considering the deleterious nature of the frameshift mutation, our study further confirmed a causative role for the *PTCH2* mutation in NBCCS. The absence of typical phenotypes in this case such as palmar/plantar pits, macrocephaly, falx calcification, hypertelorism and coarse face, together with previously reported cases, suggested that individuals with NBCCS carrying a *PTCH2* mutation may have a milder phenotype than those with a *PTCH1* mutation.

Keywords Nevoid basal cell carcinoma syndrome · *PTCH1* · *PTCH2* · Frameshift mutation

K. Fujii · T. Shiohama · H. Uchikawa
Department of Pediatrics, Chiba University Graduate School of Medicine, Chiba 260-8670, Japan

H. Ohashi
Division of Medical Genetics, Saitama Children's Medical Center, Saitama 339-8551, Japan

M. Suzuki · H. Hatsuse · T. Miyashita (✉)
Department of Molecular Genetics, Kitasato University Graduate School of Medical Sciences, 1-15-1 Kitasato, Minami-ku, Sagamihara 252-0374, Japan
e-mail: tmiyashi@med.kitasato-u.ac.jp

Introduction

Nevoid basal cell carcinoma syndrome (NBCCS) (OMIM 109400), also known as Gorlin syndrome, is an autosomal dominant disorder characterized by developmental defects including bifid ribs, palmar or plantar pits, and tumorigenesis such as the development of basal cell carcinoma, medulloblastoma, or keratocystic odontogenic tumor (KCOT) (formerly known as odontogenic keratocysts) [1]. It is transmitted with complete penetrance and variable expressivity. The gene responsible for NBCCS is the human homologue of the *Drosophila patched* gene, *PTCH1* [2, 3]. The human *PTCH1* gene contains 23 coding exons spanning approximately 70 kb and encodes a protein of 1,447 amino-acid residues containing 12 transmembrane-spanning domains and two large extracellular loops [2]. The PTCH1 protein is the ligand-binding component of the sonic hedgehog (Shh) receptor complex. In the absence of Shh binding, PTCH1 is thought to hold smoothened (SMO), a 7-pass transmembrane protein, in an inactive state and thus inhibit signaling to downstream genes. Upon the binding of Shh, the inhibition of SMO is released and signaling is transduced leading to the activation of target genes by the Gli family of transcription factors [4]. Therefore, aberrant activation of the Shh signaling cascade due to the haploinsufficiency of *PTCH1* is believed to cause NBCCS.

In vertebrates, there exists a close homolog of *PTCH1* named *PTCH2*. The human *PTCH2* gene contains 22 coding exons spanning approximately 15 kb and encodes a protein of 1,203 amino-acid residues [5]. Recently, in six affected members of a Chinese Han family with NBCCS, Fan et al. identified a heterozygous germline missense mutation in the *PTCH2* gene [6]. Here we report a case with NBCCS carrying a frameshift mutation due to a 2-bp

Published online: 12 March 2013

deletion in *PTCH2*. To our knowledge, this is the first report of NBCCS caused by a frameshift mutation and the second report of a germline mutation in the *PTCH2* gene.

Clinical report

A 13-year-old Japanese girl was referred to our hospital with jaw cysts and a rib abnormality. She was born weighing 2,570 g, with a height of 48 cm and a head circumference of 32 cm. Her two siblings as well as her parents exhibited no similar features. No consanguineous marriage was noticed in her pedigree. At 10 years of age, she had multiple KCOTs (Fig. 1a) and underwent a surgical operation to remove them. At 12 years of age, she exhibited proteinuria, and was diagnosed as having chronic glomerular nephritis. Then, she was referred to our hospital for further investigation. At examination, she was 150.1 cm tall (mean) and weighed 57.8 kg (+1.8SD). Her head circumference was 54.6 cm (mean). She had normal intelligence without neurological deficit. She exhibited no structural abnormalities of face, oral cavity, or limbs. However, chest roentgenogram revealed a left bifid rib without any other bone abnormalities (Fig. 1b). She did not exhibit palmar or plantar pits, falx calcification, medulloblastomas, or basal cell carcinomas at that time. Since she exhibited KCOTs and a rib anomaly fulfilling the diagnostic criteria made by Kimonis et al. (two major criteria), we diagnosed her as having NBCCS.

Methods

DNA extraction and PCR-sequencing analysis

All experiments described below were approved by the ethics committee at Kitasato University. DNA was extracted from peripheral blood lymphocytes using a QIAamp DNA blood midi kit (QIAGEN). The complete coding region of the *PTCH1*, *PTCH2*, suppressor of fused (*SUFU*) and *SMO* genes, including all splice junctions, was amplified from constitutional DNA as described previously [7]. Primers used for amplifying *PTCH1*, *PTCH2* and *SUFU* exons were described previously [5, 7, 8]. Those used for amplifying *SMO* are listed in supporting information Table 1. Amplified products were gel-purified using a QIAEX II gel extraction kit (QIAGEN) and cycle sequenced with a BigDye Terminator v3.1 Cycle Sequencing Kit (Applied Biosystems) in both directions. The sequence was analyzed on a 3130 Genetic Analyzer (Applied Biosystems).

Comparison of clinical manifestations

Details of a nationwide survey of NBCCS performed in Japan have been described previously [9]. The survey covered 157 NBCCS patients whose clinical details were available. Major and minor criteria for NBCCS proposed by Kimonis et al. [10] were evaluated in these patients and compared with those observed in patients carrying a *PTCH2* mutation reported previously including the present case [6].

Results

No mutation in *PTCH1* or the related genes *SUFU* and *SMO* was detected in the peripheral blood from this patient. Although deletion of the entire *PTCH1* gene is a common event in point mutation-negative cases of NBCCS as we reported previously [11], no such deletion was observed using either a ligation-dependent probe amplification method or high-resolution array-based comparative genomic hybridization technology [11–13]. We then sequenced all exons of the *PTCH2* gene, since *PTCH2* is a close homolog of *PTCH1* and is also a suppressor component of the Shh pathway. As a result, a heterozygous 2-base-pair deletion, c.1172_1173delCT, was detected in exon 9 of *PTCH2* (Fig. 2). This mutation caused a frameshift and created a premature termination codon (PTC) at the site of the deletion resulting in a truncated form of the PTCH2 protein, p.S391X.

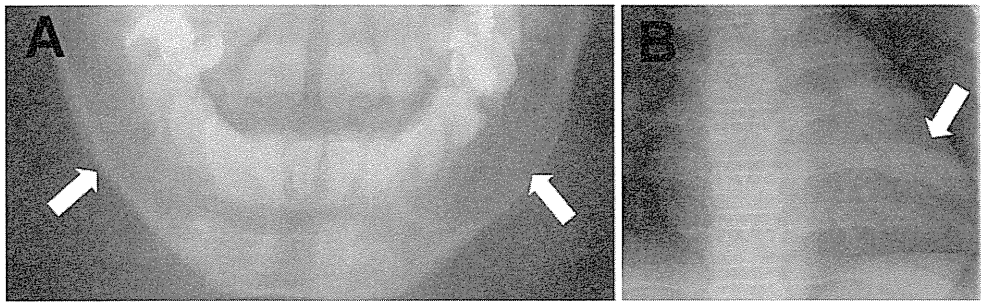

Fig. 1 Roentgenograms of the patient. **a** Pantomography shows bilateral keratocystic odontogenic tumors (*Arrows*). **b** Chest roentgenogram reveals a bifid anomaly of the left sixth rib (*Arrow*)

Table 1 Comparison of the characteristic phenotype of NBCCS in three groups

Patients	Number of patients	Mean age	Mean number of major criteria	Mean number of minor criteria
Nationwide survey	157	33.1	2.4*	1.3**
With *PTCH2* mutation	7	34.1	1.57	0.14

*$P < 0.05$ (vs *PTCH2* mutation), ** $P < 0.01$ (vs *PTCH2* mutation)

In order to characterize the phenotype of individuals carrying a *PTCH2* mutation, we next evaluated the number of positive criteria for NBCCS proposed by Kimonis et al. [10] in two groups; first, NBCCS patients collected by a nationwide survey described previously [9], second, reported individuals carrying a *PTCH2* mutation including our case. In spite of the comparable mean ages in two groups (33.1 vs 34.1 years old), positivities of most of the criteria were lower in the *PTCH2* mutation-positive group than in the other, indicating that *PTCH2* mutations cause a milder phenotype than the classical NBCCS (Table 1). In fact, only 4 out of 7 individuals in the *PTCH2* mutation-positive group diagnosed as having NBCCS according to this diagnostic criteria.

Discussion

NBCCS is caused by a mutation in the gene *PTCH1*, with rare exceptions in which a *SUFU* mutation has been identified [8, 14, 15]. Recently, a heterozygous missense mutation in the *PTCH2* gene, c.2157G>A (p.R719Q), was identified in 6 affected members of a Chinese Han family with NBCCS [6]. Although the pathological significance of missense mutations should be discussed cautiously, this mutation was demonstrated to result in the inactivation of PTCH2's inhibitory activities at least in vitro. In this paper, we reported a second germline mutation of *PTCH2*, c.1172_1173delCT, found in a Japanese patient with NBCCS. This mutation created a PTC at the site of the deletion in the mutant allele, resulting in the truncation of the PTCH2 protein. However, since the PTC leads to the degradation of mRNA via a mechanism called nonsense-mediated mRNA decay [16], a haploinsufficiency of *PTCH2* is expected to play an important role in this case.

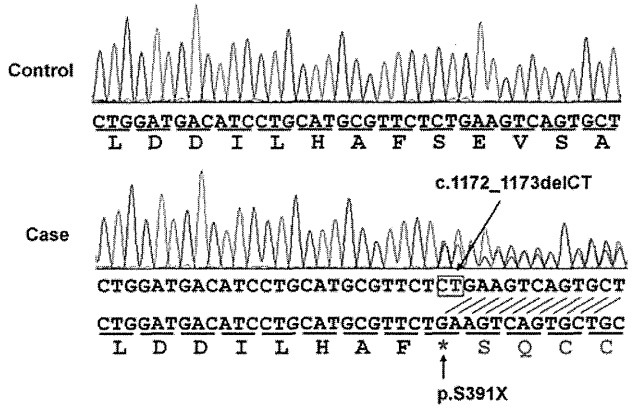

Fig. 2 Electropherograms of the *PTCH2* exon 9 sequence. DNA extracted from the peripheral blood of the patient (Case) as well as a healthy control (Control) was subjected to PCR direct sequencing. The predicted translation is indicated at the bottom of each electropherogram. PTC created by the deletion is indicated by an *asterisk*

Interestingly, this mutation is also present in the dbSNP database as rs56126236, submitted by the Center for Genome Medicine, Kyoto University Graduate School of Medicine, Japan. However, details such as frequency are unclear. Therefore, we analyzed 63 healthy Japanese individuals (126 alleles) on this mutation, but found none carrying this deletion. Thus, it is unlikely that this is a rare polymorphism at least in a Japanese population.

However, unfortunately, we were unable to get informed consents from family members and, therefore, could not add data regarding this issue. Nonetheless, considering the deleterious nature of the mutation, we believe that the mutation found in this patient is generated de novo.

Homozygous mutant mice, *Ptch2*$^{-/-}$, developed normally, were viable and fertile, and did not display any obvious defects in hair follicle, limb, neural, or testis development [17]. However, with age, homozygous mutant male mice developed skin lesions consisting of alopecia and epidermal hyperplasia, suggesting a role for *Ptch2* in adult epidermal homeostasis via Shh signaling. In accordance with the milder phenotype of *Ptch2*$^{-/-}$ than *Ptch1*$^{-/-}$, which is embryonic lethal [18], it is not surprising that individuals carrying a *PTCH2* mutation also exhibit milder clinical manifestations than those with classical NBCCS. Our patient lacked typical NBCCS phenotypes such as palmar/plantar pits, falx calcification, macrocephaly, hypertelorism and coarse face, the frequencies of which are 60.1, 79.6, 26.5, 68.8, and 27.9 %, respectively, in the Japanese population [9]. In fact, this case does not fulfill the criteria by Evans et al. [19] because a rib anomaly is considered to be a minor criterion. Since the number of cases with a *PTCH2* mutation is still limited, the accumulation of such patients is expected to further clarify their characteristic phenotype.

A genotype–phenotype correlation has not been reported in NBCCS patients [20]. However, mutations in the *SUFU*

gene were reported to result in a much higher incidence of medulloblastoma than those in *PTCH1* [8, 14, 21]. It is also reported that a large genomic deletion encompassing *PTCH1* leads to NBCCS with atypical clinical manifestations, probably due to a deletion of adjacent gene(s) [12]. Therefore, it should be noted that NBCCS cases caused by a mutation of a gene other than *PTCH1* have phenotypes different from those of classical NBCCS caused by *PTCH1* mutations.

Acknowledgments This research was supported by Science Research Grants for intractable diseases in Japan (H22-intractable diseases-120) from the Ministry of Health, Labour and Welfare, and by a Grant-in-Aid for Scientific Research (20591261) from the Ministry of Education, Culture, Sports, Science and Technology.

Conflict of interest The authors declare that they have no conflict of interest.

References

1. Gorlin RJ (1987) Nevoid basal-cell carcinoma syndrome. Medicine (Baltimore) 66:98–113
2. Johnson RL, Rothman AL, Xie J, Goodrich LV, Bare JW, Bonifas JM, Quinn AG, Myers RM, Cox DR, Epstein EH Jr, Scott MP (1996) Human homolog of *patched*, a candidate gene for the basal cell nevus syndrome. Science 272:1668–1671
3. Hahn H, Wicking C, Zaphiropoulous PG, Gailani MR, Shanley S, Chidambaram A, Vorechovsky I, Holmberg E, Unden AB, Gillies S, Negus K, Smyth I, Pressman C, Leffell DJ, Gerrard B, Goldstein AM, Dean M, Toftgard R, Chenevix-Trench G, Wainwright B, Bale AE (1996) Mutations of the human homolog of Drosophila *patched* in the nevoid basal cell carcinoma syndrome. Cell 85:841–851
4. Ingham PW, McMahon AP (2001) Hedgehog signaling in animal development: paradigms and principles. Genes Dev 15:3059–3087
5. Smyth I, Narang MA, Evans T, Heimann C, Nakamura Y, Chenevix-Trench G, Pietsch T, Wicking C, Wainwright BJ (1999) Isolation and characterization of human *patched 2* (*PTCH2*), a putative tumour suppressor gene in basal cell carcinoma and medulloblastoma on chromosome 1p32. Hum Mol Genet 8:291–297
6. Fan Z, Li J, Du J, Zhang H, Shen Y, Wang CY, Wang S (2008) A missense mutation in PTCH2 underlies dominantly inherited NBCCS in a Chinese family. J Med Genet 45:303–308
7. Fujii K, Kohno Y, Sugita K, Nakamura M, Moroi Y, Urabe K, Furue M, Yamada M, Miyashita T (2003) Mutations in the human homologue of *Drosophila patched* in Japanese nevoid basal cell carcinoma syndrome patients. Hum Mutat 21:451–452
8. Kijima C, Miyashita T, Suzuki M, Oka H, Fujii K (2012) Two cases of nevoid basal cell carcinoma syndrome associated with meningioma caused by a *PTCH1* or *SUFU* germline mutation. Fam Cancer 11:565–570
9. Endo M, Fujii K, Sugita K, Saito K, Kohno Y, Miyashita T (2012) Nationwide survey of nevoid basal cell carcinoma syndrome in Japan revealing the low frequency of basal cell carcinoma. Am J Med Genet A 158A:351–357
10. Kimonis VE, Goldstein AM, Pastakia B, Yang ML, Kase R, DiGiovanna JJ, Bale AE, Bale SJ (1997) Clinical manifestations in 105 persons with nevoid basal cell carcinoma syndrome. Am J Med Genet 69:299–308
11. Nagao K, Fujii K, Saito K, Sugita K, Endo M, Motojima T, Hatsuse H, Miyashita T (2011) Entire PTCH1 deletion is a common event in point mutation-negative cases with nevoid basal cell carcinoma syndrome in Japan. Clin Genet 79:196–198
12. Fujii K, Ishikawa S, Uchikawa H, Komura D, Shapero MH, Shen F, Hung J, Arai H, Tanaka Y, Sasaki K, Kohno Y, Yamada M, Jones KW, Aburatani H, Miyashita T (2007) High-density oligonucleotide array with sub-kilobase resolution reveals breakpoint information of submicroscopic deletions in nevoid basal cell carcinoma syndrome. Hum Genet 122:459–466
13. Kosaki R, Nagao K, Kameyama K, Suzuki M, Fujii K, Miyashita T (2012) Heterozygous tandem duplication within the *PTCH1* gene results in nevoid basal cell carcinoma syndrome. Am J Med Genet A 158A:1724–1728
14. Taylor MD, Liu L, Raffel C, Hui CC, Mainprize TG, Zhang X, Agatep R, Chiappa S, Gao L, Lowrance A, Hao A, Goldstein AM, Stavrou T, Scherer SW, Dura WT, Wainwright B, Squire JA, Rutka JT, Hogg D (2002) Mutations in SUFU predispose to medulloblastoma. Nat Genet 31:306–310
15. Pastorino L, Ghiorzo P, Nasti S, Battistuzzi L, Cusano R, Marzocchi C, Garre ML, Clementi M, Scarra GB (2009) Identification of a SUFU germline mutation in a family with Gorlin syndrome. Am J Med Genet A 149A:1539–1543
16. Holbrook JA, Neu-Yilik G, Hentze MW, Kulozik AE (2004) Nonsense-mediated decay approaches the clinic. Nat Genet 36: 801–808
17. Nieuwenhuis E, Motoyama J, Barnfield PC, Yoshikawa Y, Zhang X, Mo R, Crackower MA, Hui CC (2006) Mice with a targeted mutation of patched2 are viable but develop alopecia and epidermal hyperplasia. Mol Cell Biol 26:6609–6622
18. Goodrich LV, Milenkovic L, Higgins KM, Scott MP (1997) Altered neural cell fates and medulloblastoma in mouse patched mutants. Science 277:1109–1113
19. Evans DG, Ladusans EJ, Rimmer S, Burnell LD, Thakker N, Farndon PA (1993) Complications of the naevoid basal cell carcinoma syndrome: results of a population based study. J Med Genet 30:460–464
20. Wicking C, Shanley S, Smyth I, Gillies S, Negus K, Graham S, Suthers G, Haites N, Edwards M, Wainwright B, Chenevix-Trench G (1997) Most germ-line mutations in the nevoid basal cell carcinoma syndrome lead to a premature termination of the PATCHED protein, and no genotype–phenotype correlations are evident. Am J Hum Genet 60:21–26
21. Brugieres L, Pierron G, Chompret A, Paillerets BB, Di Rocco F, Varlet P, Pierre-Kahn A, Caron O, Grill J, Delattre O (2010) Incomplete penetrance of the predisposition to medulloblastoma associated with germ-line SUFU mutations. J Med Genet 47:142–144

Congenital Anomalies
THE JAPANESE TERATOLOGY SOCIETY
doi:10.1111/j.1741-4520.2012.00362.x
Congenital Anomalies 2013; **53**, 49–53

CASE REPORT

Patient with terminal 9 Mb deletion of chromosome 9p: Refining the critical region for 9p monosomy syndrome with trigonocephaly

Norimasa Mitsui[1], Kenji Shimizu[2], Hiroshi Nishimoto[3], Hiroshi Mochizuki[4], Masao Iida[1], and Hirofumi Ohashi[2]
[1]Department of Clinical Laboratory, Divisions of [2]Medical Genetics, [3]Neurosurgery, and [4]Metabolism and Endocrinology, Saitama Children's Medical Center, Saitama, Japan

ABSTRACT **We describe a patient with typical manifestations of 9p monosomy syndrome, including trigonocephaly and sex reversal. Array comparative genomic hybridization (CGH) revealed a 9p terminal deletion of approximately 9 Mb with the breakpoint at 9p23. We compared the deleted segments of 9p associated with reported cases of 9p monosomy syndrome with trigonocephaly. We did not identify a region that was shared by all patients; however, when only pure terminal or interstitial deletions that did not involve material from any other chromosome were compared, we identified a segment from D9S912 to RP11-439I6 of approximately 1 Mb that was deleted in every patient. We propose that this 1-Mb segment might be the critical region for 9p monosomy syndrome with trigonocephaly.**

Key Words: 9p monosomy, craniosynostosis, critical region, sex reversal, trigonocephaly

INTRODUCTION

Monosomy 9p syndrome [MIM 158170] is a rare but well-known chromosomal deletion syndrome characterized by distinct craniofacial features (including trigonocephaly), various systemic anomalies, developmental retardation, and occasional sex reversal in XY patients (Huret et al. 1988). Since Alfi et al. (1973) first described a patient with the syndrome, more than 100 patients, most with terminal deletions with breakpoints around 9p21-p23 based on chromosome G-band analysis, have been reported. Recent advances in molecular/cytogenetic techniques allow attempts to map the loci responsible for cardinal features of the syndrome, especially trigonocephaly and sex reversal. While *DMRT* genes, which map to the most terminal 9p24.3 band, have been elucidated as the genes responsible for sex reversal (Raymond et al. 1998; Ogata et al. 2001; Barbaro et al. 2009), no gene has yet been identified as definitively responsible for trigonocephaly. Moreover, previous studies have been inconsistent with regard to identification of the 9p regions that are responsible for trigonocephaly (Wagstaff and Hemann 1995; Christ et al. 1999; Kawara et al. 2006; Faas et al. 2007; Hauge et al. 2008; Swinkels et al. 2008; Shimojima and Yamamoto 2009). Here, we describe a patient with a terminal 9p deletion of approximately 9 Mb who has the typical clinical manifestations of 9p monosomy syndrome, including trigonocephaly and sex reversal.

Correspondence: Hirofumi Ohashi, MD, PhD, Division of Medical Genetics, Saitama Children's Medical Center, 2100 Magome, Iwatsuki-ku, Saitama-shi, Saitama 339-8551, Japan. Email: ohashi.hirofumi@pref.saitama.lg.jp

Received January 20, 2012; revised and accepted February 9, 2012.

CLINICAL REPORT

The girl patient was born by cesarean section after 38-week gestation to a 30-year-old gravida 2, para 1 mother and a 31-year-old father, both Japanese, healthy, and unrelated. The patient's birth weight was 2864 g (−0.5 SD), length 49.5 cm (+0.2 SD), and occipitofrontal head circumference 35.5 cm (+1.5 SD). The patient had a healthy older sister. The patient was referred to us at the age of 11 months because of developmental delay and skull deformity. The notable craniofacial features were trigonocephaly, ptosis of the eyelids, epicanthus, upslanting palpebral fissures, flat nasal bridge, broad nasal root, long philtrum, thin upper lip, and low-set ears. A skull computed tomography scan with 3D reconstruction confirmed trigonocephaly with metopic suture synostosis (Fig. 1). Frontoorbital advancement with cranial reshaping was performed when she was 1 year and 3 months old. She showed normal female external genitalia. When the patient was 2 years old, an abdominal ultrasonography revealed a uterus, but no ovary or testis was detected. A test of human chorionic gonadotropin load suggested the existence of testis, while luteinizing hormone-releasing hormone load test revealed primary hypogonadism. She weighed 14 kg (−1.7 SD) and was 100.2 cm tall (−1.9 SD) at 5 years of age. Her development was moderately delayed, and her IQ was estimated to be around 40 with the Tanaka–Binet Intelligence Scale at the age of 6 years.

G-banding analysis at a resolution of 550-bands on metaphase chromosomes obtained from phytohemagglutinin-stimulated lymphocyte cultures from the patient revealed a distal deletion of the short arm of chromosome 9 with a breakpoint at 9p23 and an XY sex chromosome constitution (sex reversal) (Fig. 2). Her parents were chromosomally normal. Fluorescence *in situ* hybridization (FISH) using whole-chromosome painting probes for chromosome 9 and a subtelomeric probe for the short arm of chromosome 9 (both from Vysis/Abbott Molecular Inc., Des Plaines, IL, USA) revealed that the abnormal chromosome 9 did not contain translocated material from another chromosome. To further define the extent of the deleted region in 9p, we performed an array comparative genomic hybridization (CGH) analysis using the Agilent Human Genome 244 K CGH kit (Agilent Technologies, Santa Clara, CA, USA). The result showed a hemizygous 9.17 Mb terminal deletion of chromosome 9p and no other apparent pathogenic copy number variation was identified in the whole genome (Fig. 3). Her karyotype was designated as 46,XY,del(9)(p23).arr 9p23 (194 193-9 169 072)x1 dn. FISH analyses with bacterial artificial chromosome (BAC) clones spanning the region from 9p23 to 9p24 refined the breakpoint between the clones RP11-1134E16 (D9S2000) and RP11-74 L16 (D9S912) (Table 1). BACs containing *DMRT1* and *DMRT2*, both candidate genes for sex reversal (9p24.3), were confirmed to be in the deleted segment of 9p in the patient.

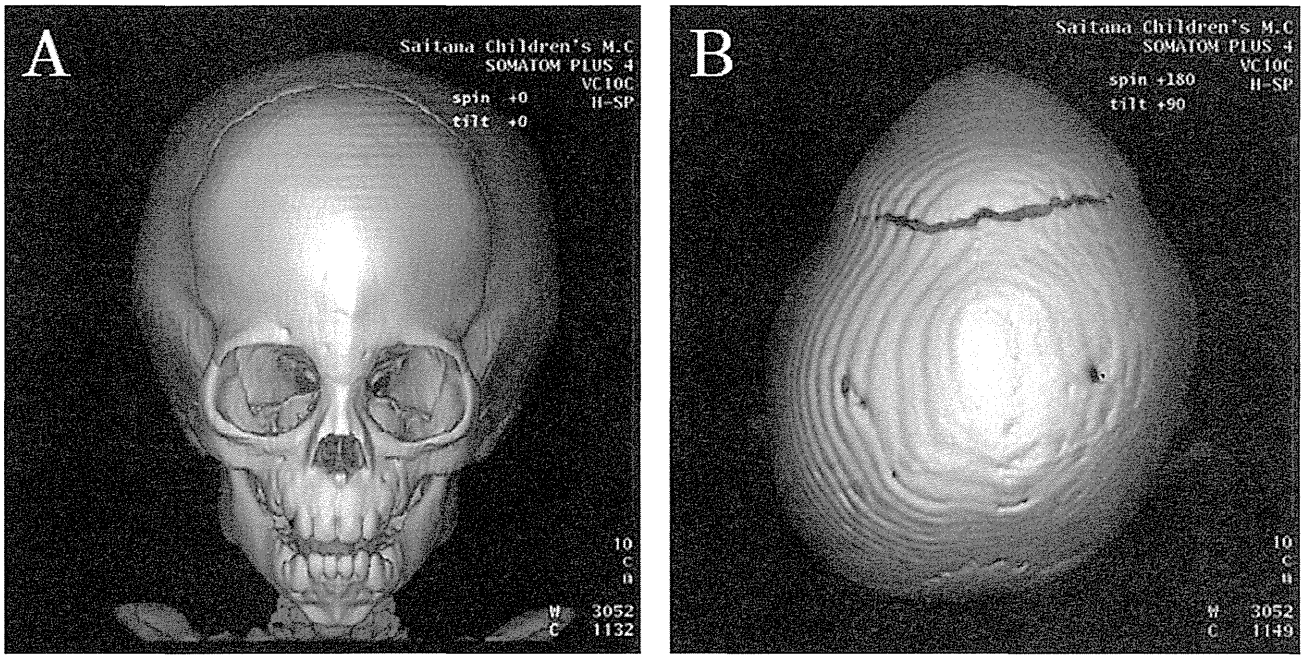

Fig. 1 Frontal (a) and top (b) views of the skull of the patient at age 11 months showing trigonocephaly, reconstructed by three-dimensional computed tomography.

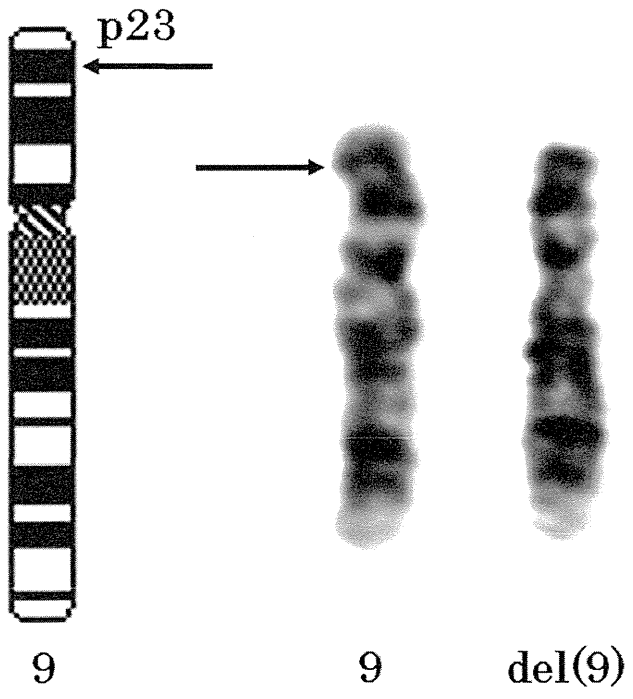

Fig. 2 G-banded partial karyotype of the patient showing a terminal deletion of chromosome 9. Arrow indicates the deletion breakpoint.

DISCUSSION

We described herein a girl patient with a terminal deletion of the short arm of chromosome 9 who had full manifestations of monosomy 9p syndrome, including distinctive craniofacial features (e.g. trigonocephaly, ptosis of the eyelids, epicanthus, upslanting palpebral fissures, flat nasal bridge, broad nasal root, low-set ears, long philtrum, thin upper lip), developmental delay, and XY sex reversal. Array CGH and FISH analyses revealed a pure terminal 9p deletion of approximately 9 Mb with the breakpoint between RP11-1134E16 and RP11-74 L16 at 9p23. *DMRT* genes, candidates for sex reversal (9p24.3), were included in the deletion in this patient.

Since Alfi et al. (1973) first reported 9p monosomy syndrome it has been established as a chromosomal deletion syndrome on the basis of G-banding cytogenetic analysis. Breakpoints in most patients with the syndrome, either with a pure terminal deletion or with a deletion associated with an unbalanced chromosome segment, reside around band 9p21-p23 (Huret et al. 1988). Recent advances in molecular techniques have allowed us to study precise correlations between the phenotype and karyotype/genotype associated with this syndrome. Wagstaff and Hemann (1995) first defined the critical region for 9p monosomy syndrome, including trigonocephaly, based on a boy with cryptic 9p monosomy, who was found to have a 9p deletion of approximately 11.6 Mb that included the region from D9S286 (9p24.1) to D9S162 (9p22.1); this deletion was associated with a translocation between 3p and 9p. Christ et al. (1999) studied 24 patients with 9p deletions (terminal deletions with or without unbalanced translocation), all of whom showed the consensus 9p-deletion phenotype (including trigonocephaly), and found that the minimum common deleted region is 16.1 Mb from D9S285 to the 9p terminal. Subsequently, several reports have been published that further define the critical region for the syndrome (Kawara et al. 2006; Faas et al. 2007; Hauge et al. 2008; Swinkels et al. 2008; Shimojima and Yamamoto 2009). Although, along with these works, some genes such as *CER1*, *TYRP1* and *PTPRD* have been postulated as possible candidate genes, no gene has yet been identified as conclusively responsible for the syndrome (Shimojima and Yamamoto 2009).

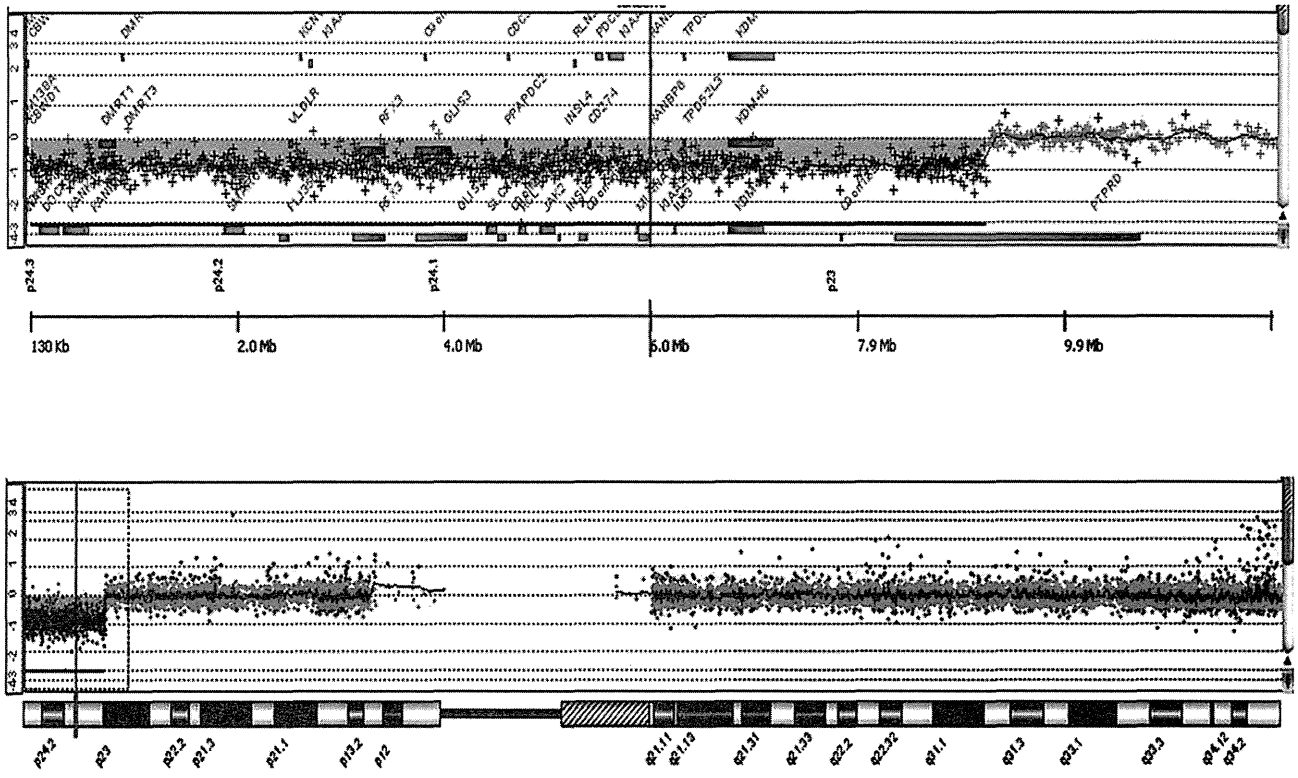

Fig. 3 Oligonucleotide array-CGH result of the patient. Whole chromosome view (lower) and close view (upper) of chromosome 9. Note a loss of 9.17 Mb of the terminal region of chromosome 9p.

Table 1 Fluoresence in situ hybridization (FISH) results using bacterial artificial chromosome clones and a subtelomeric probe around distal 9p

Probe name	Locus	Chromosome band	Distance from 9p terminal(Mb)	Signal on del(9p)
9p subtelomeric probe	–	9p24.3	–	–
RP11-143 M15	DMRT1	9p24.3	0.81	–
RP11-590E10	DMRT2	9p24.3	0.97	–
RP11-79 K3	–	9p24.1	7.30	–
RP11-29B9	D9S286	9p24.1	7.90	–
RP11-1134E16	D9S2000	9p23	8.99	–
RP11-74 L16	D9S912	9p23	9.26	+
RP11-176P17	D9S144	9p23	9.50	+
RP11-87N24	D9S168	9p23	10.47	+
RP11-58B8	–	9p23	11.60	+
RP11-382H24	D9S267	9p23	13.00	+

The distance from 9p terminal was retrieved from UCSC Genome Browser (NCBI 36/hg 18).

We compared deleted segments in all reported cases of 9p monosomy that were evaluated using molecular techniques (Fig. 4). Patients without trigonocephaly were not included in this comparison because penetrance of trigonocephaly might not be 100% and therefore considered unsuitable for use in phenotype mapping. While we could not find a common region that was shared by all patients, the segment from D9S912 to RP11-439I6, which is approximately 1 Mb, was deleted in the vast majority of the patients. There are only two patients who have a deletion that does not include this 1-Mb segment. The case reported by Kawara et al. (2006) had a more proximal interstitial deletion of 4.7 Mb at 9p22.3-p23. The chromosomal rearrangement in this patient was highly complex and

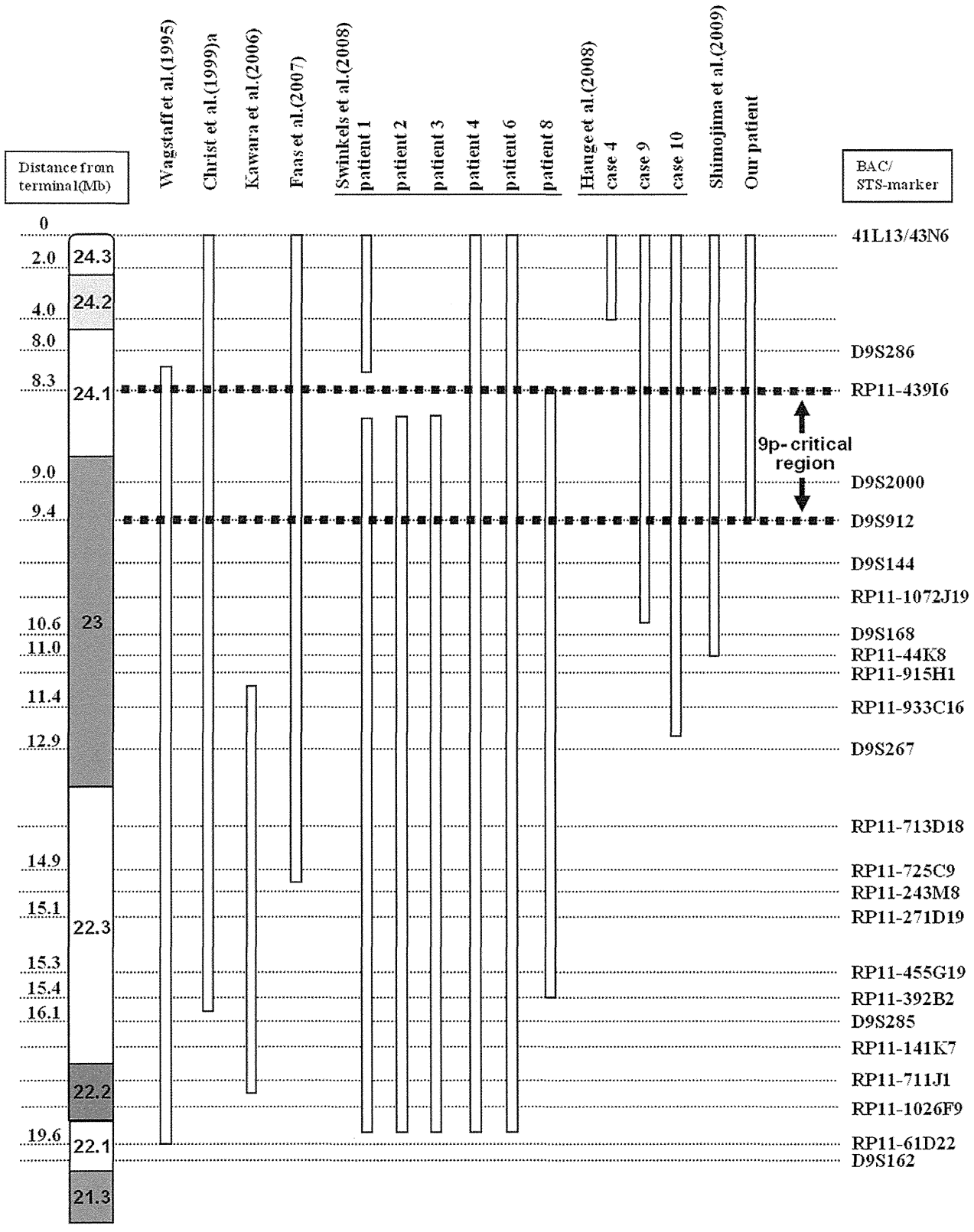

Fig. 4 Schematic map of the 9p deletion of reported cases of 9p monosomy, including the present case, evaluated using molecular analyses such as fluoresence in situ hybridization (FISH) and/or array comparative genomic hybridization. Open bars represent the presumed maximum extent of the deletion in each patient. a: the minimum common deleted region shared by 24 patients.

involved seven breakpoints on chromosomes 2 and 9. The patient, Case 4, reported by Hauge et al. (2008) showed a tiny terminal deletion of no more than 4 Mb. The karyotype of this patient was der(9)t(9;15) with a trisomic region from 15q(15q25-qter) that was translocated onto 9p24. That these two patients did not carry pure deletions of 9p may be noteworthy. Complex chromosome rearrangements are likely to have cryptic genome imbalance not only around the breakpoints but also at regions apart from the breakpoints. The altered chromosome constitution associated with unbalanced translocations might influence gene expression on the derivative chromosomes possibly through epigenetic modifications (Harewood et al. 2010). Obviously, it is preferable to choose pure terminal or interstitial deletion patients for genotype-phenotype mapping. In view of this preference and on the basis of comparison of deleted segments among patients with pure terminal or interstitial 9p deletion, including the present patient, we suggest the critical region for 9p monosomy syndrome, including trigonocephaly, might be a segment from D9S912 to RP11-439I6 of approximately 1 Mb. Of course, there are other possibilities: (i) the presence of multiple loci responsible for the syndrome and (ii) the presence of modifying factors that are located in different regions of the genome (Hauge et al. 2008). Further studies, such as using exome sequencing to screen cytogenetically normal patients with the 9p monosomy syndrome phenotype or with isolated trigonocephaly, might be necessary to identify the responsible gene for trigonocephaly of the 9p monosomy syndrome.

ACKNOWLEDGMENT

This study was funded in part by a grant from the Ministry of Health, Labour and Welfare, Japan, and from Kawano Masanori Memorial Foundation for Promotion of Pediatrics.

REFERENCES

Alfi O, Donnell GN, Crandall BF, Derencsenyi A, Menon R. 1973. Deletion of the short arm of chromosome no.9 (46,9p-): a new deletion syndrome. Ann Genet 16:17–22.

Barbaro M, Balsamo A, Anderlid BM et al. 2009. Characterization of deletions at 9p affecting the candidate regions for sex reversal and deletion 9p syndrome by MLPA. Eur J Hum Genet 17:1439–1447.

Christ LA, Crowe CA, Micale MA, Conroy JM, Schwartz S. 1999. Chromosome breakage hotspots and delineation of the critical region for the 9p-deletion syndrome. Am J Hum Genet 65:1387–1395.

Faas BH, de Leeuw N, Mieloo H, Bruinenberg J, de Vries BB. 2007. Further refinement of the candidate region for monosomy 9p syndrome. Am J Med Genet A 143A:2353–2356.

Harewood L, Schutz F, Boyle S et al. 2010. The effect of translocation-induced nuclear reorganization on gene expression. Genome Res 20:554–564.

Hauge X, Raca G, Cooper S et al. 2008. Detailed characterization of, and clinical correlations in, 10 patients with distal deletions of chromosome 9p. Genet Med 10:599–611.

Huret JL, Leonard C, Forestier B, Rethore MO, Lejeune J. 1988. Eleven new cases of del(9p) and features from 80 cases. J Med Genet 25:741–749.

Kawara H, Yamamoto T, Harada N et al. 2006. Narrowing candidate region for monosomy 9p syndrome to a 4.7-Mb segment at 9p22.2-p23. Am J Med Genet A 140:373–377.

Ogata T, Muroya K, Ohashi H, Mochizuki H, Hasegawa T, Kaji M. 2001. Female gonadal development in XX patients with distal 9p monosomy. Eur J Endocrinol 145:613–617.

Raymond CS, Shamu CE, Shen MM et al. 1998. Evidence for evolutionary conservation of sex-determining genes. Nature 391:691–695.

Shimojima K, Yamamoto T. 2009. Investigation of the candidate region for trigonocephaly in a patient with monosomy 9p syndrome using array-CGH. Am J Med Genet A 149A:1076–1080.

Swinkels ME, Simons A, Smeets DF et al. 2008. Clinical and cytogenetic characterization of 13 Dutch patients with deletion 9p syndrome: delineation of the critical region for a consensus phenotype. Am J Med Genet A 146A:1430–1438.

Wagstaff J, Hemann M. 1995. A familial 'balanced' 3;9 translocation with cryptic 8q insertion leading to deletion and duplication of 9p23 loci in siblings. Am J Hum Genet 56:302–309.

Focal Segmental Glomerulosclerosis in Patients With Complete Deletion of One *WT1* Allele

AUTHORS: Kazumoto Iijima, MD, PhD,[a] Tomonosuke Someya, MD, PhD,[b] Shuichi Ito, MD, PhD,[c] Kandai Nozu, MD, PhD,[a] Koichi Nakanishi, MD, PhD,[d] Kentaro Matsuoka, MD, PhD,[e] Hirofumi Ohashi, MD, PhD,[f] Michio Nagata; MD, PhD,[g] Koichi Kamei, MD, PhD,[c] and Satoshi Sasaki, MD, PhD[h]

[a]Department of Pediatrics, Kobe University Graduate School of Medicine, Kobe, Japan; [b]Department of Pediatrics, Juntendo University School of Medicine, Tokyo, Japan; [c]Departments of Nephrology and Rheumatology, and [e]Pathology, National Center for Child Health and Development, Tokyo, Japan; [d]Department of Pediatrics, Wakayama Medical University, Wakayama, Japan; [f]Division of Medical Genetics, Saitama Children's Medical Center, Saitama, Japan; [g]Department of Pathology, Institute of Basic Medical Sciences, University of Tsukuba, Tsukuba, Japan; and [h]Department of Pediatrics, Hokkaido University Graduate School of Medicine, Sapporo, Japan

KEY WORDS
deletion, focal segmental glomerulosclerosis, WAGR syndrome, *WT1*

ABBREVIATIONS
ACEI—angiotensin-converting enzyme inhibitor
BUN—blood urea nitrogen
CrCl—creatinine clearance
DDS—Denys-Drash syndrome
DMS—diffuse mesangial sclerosis
FSGS—focal segmental glomerulosclerosis
WAGR—Wilms' tumor, aniridia, genitourinary anomalies, and mental retardation

Each author contributed to the study as follows: Dr Iijima, patient management and manuscript writing; Dr Someya, patient management; Dr Ito, patient management; Dr Nozu, genetic analysis; Dr Nakanishi, genetic analysis; Dr Matsuoka, pathological analysis; Dr Ohashi, genetic analysis; Dr Nagata, pathological analysis; Dr Kamei, patient management; and Dr Sasaki, patient management.

www.pediatrics.org/cgi/doi/10.1542/peds.2011-1323

doi:10.1542/peds.2011-1323

Accepted for publication Jan 11, 2012

Address correspondence to Kazumoto Iijima, MD, PhD, Department of Pediatrics, Kobe University Graduate School of Medicine, 7-5-2 Kusunoki-Cho, Chuo-ku, Kobe 650–0017, Japan. E-mail: iijima@med.kobe-u.ac.jp

PEDIATRICS (ISSN Numbers: Print, 0031-4005; Online, 1098-4275).

FINANCIAL DISCLOSURE: *The authors have indicated they have no financial relationships relevant to this article to disclose.*

FUNDING: This study was supported by Grants-in-Aid for Scientific Research (B) (to Dr Iijima, 20390240) from the Japan Society for the Promotion of Science.

abstract

The renal prognosis of patients with Wilms' tumor, aniridia, genitourinary anomalies, and mental retardation syndrome (WAGR) is poor. However, the renal histology and its mechanisms are not well understood. We performed renal biopsies in 3 patients with WAGR syndrome who had heavy proteinuria. The complete deletion of one *WT1* allele was detected in each patient by constitutional chromosomal deletion at 11p13 using G-banding, high-resolution G-banding, and fluorescence in situ hybridization. The patients exhibited proteinuria at the ages of 6, 10, and 6 years and were diagnosed as having focal segmental glomerulosclerosis (FSGS) at the ages of 7, 16 and 19 years, respectively. They exhibited normal or mildly declined renal function at the time of biopsy. Re-examination of a nephrectomized kidney from 1 patient revealed that some glomeruli showed segmental sclerosis, although he did not have proteinuria at the time of nephrectomy. The other 2 patients did not develop Wilms' tumor and thus did not undergo nephrectomy, chemotherapy, or radiotherapy, thereby eliminating any effect of these therapies on the renal histology. In conclusion, complete deletion of one *WT1* allele may induce the development of FSGS. Our findings suggest that haploinsufficiency of the *WT1* could be responsible for the development of FSGS. *Pediatrics* 2012;129:e1621–e1625

Miller et al[1] first described WAGR syndrome (Wilms' tumor, aniridia, genitourinary anomalies, and mental retardation). Children with WAGR syndrome invariably have a constitutional chromosomal deletion at 11p13, the region where the *WT1* gene is located. Patients with Denys-Drash syndrome (DDS) usually have a germline missense mutation, which is predicted to result in an amino acid substitution in the eighth or ninth exon of *WT1*. Little et al[2] suggested that the severe nephropathy associated with DDS, which frequently leads to early renal failure, might result from the dominant-negative action of altered *WT1*. By contrast, because of the less severe genital anomalies and apparent lack of nephropathy associated with WAGR, a reduced *WT1* dosage during embryogenesis is thought to have a less pronounced effect on development, especially on renal system development.[3] Breslow et al[4] reviewed nearly 6000 patients enrolled in 4 clinical trials administered by the US National Wilms Tumor Study Group between 1969 and 1995. Of 22 patients with DDS, 13 (59%) developed renal failure; of 46 patients with WAGR, 10 (22%) developed renal failure. The cumulative risks of renal failure at 20 years were 62% and 38%, respectively. These findings suggest that nephropathy is not uniquely associated with missense mutations in *WT1* and that patients with the WAGR syndrome should be followed up closely throughout life for signs of nephropathy.

The renal prognosis of patients with WAGR is poor. However, the renal histology and its mechanisms are not well understood. We therefore performed renal biopsies to reveal the renal pathology in 3 patients with WAGR syndrome who had heavy proteinuria.

CASE REPORTS

Patient 1

Patient 1 was a male diagnosed with bilateral microphthalmos at 1 month of age. Wilms' tumor developed bilaterally at 3 years of age. He also had undescended testes and mental retardation. Previous analysis of G-banded metaphase chromosomes revealed a deletion of chromosome 11p13-15.1 in one allele[5]; the diagnosis of atypical WAGR syndrome was therefore made.[6] Because of a large tumor in the right kidney after the first chemotherapy treatment, the right kidney was nephrectomized. A diagnosis of nephroblastoma (nephroblastic type) was made. At the same time, the contralateral left kidney was biopsied, but no tumor was detected. The nephrectomized kidney revealed that there were no immature glomeruli, and a few glomeruli showed segmental sclerosis (Fig 1 A and B). The patient did not have proteinuria at the time of nephrectomy although microalbuminuria could have been detected.

The patient then underwent a second session of chemotherapy and radiotherapy treatment with left kidney protection. He developed heavy proteinuria at 6 years of age. The left kidney was biopsied (open biopsy) at age 7 years. Renal biopsy findings were consistent with focal segmental glomerulosclerosis (FSGS) (Fig 1 C and D). At the time of biopsy, the patient's height was 107.3 cm (–2.9 SD), weight was 21.7 kg (–0.7 SD), and blood pressure was 120/80 mm Hg. Biochemical data were as follows: total protein, 6.5 g/dL; albumin, 3.3 g/dL; blood urea nitrogen (BUN), 12.9 mg/dL; creatinine, 0.43 mg/dL; 24-hour creatinine clearance (CrCl), 72.2 mL/min/1.73 m^2; early morning urinary protein, 3+ (as measured by using a dipstick test); urinary protein to urinary creatinine ratio, 3.6 (milligram/milligram); and urinary β-2 microglobulin, 0.44 mg/dL (normal range: <0.23 mg/dL). His renal function gradually deteriorated despite angiotensin-converting enzyme inhibitor (ACEI) treatment. At 14 years of age, he underwent a preemptive living-related renal transplantation from his father.

Patient 2

Patient 2 was a male with aniridia, bilateral undescended testes, hypospadias, grade III to IV bilateral vesicoureteral reflux, and mental retardation. High-resolution G-banding revealed deletion of chromosome 11p13-p14.2 in one allele (Fig 2A), and fluorescence in situ hybridization showed heterozygous deletions of *PAX6*, *D11S2163*, *PER*, and *WT1* (Fig 2B), indicating WAGR syndrome. He had a single febrile urinary tract infection at 2 years of age and underwent an antireflux operation at 4 years of age, which resolved his vesicoureteral reflux. A dimercaptosuccinic acid radionuclide scan showed several defects in his right kidney. His proteinuria was detected at 10 years of age by the school urinary screening program. His proteinuria gradually increased, and he underwent renal biopsy (right kidney) at age 16 years. Renal biopsy findings were consistent with FSGS (Fig 1 E and F). At the time of biopsy, the patient's height was 169.2 cm, weight was 67.4 kg, and blood pressure was 128/78 mm Hg. Biochemical data were as follows: total protein, 6.8 g/dL; albumin, 4.3 g/dL; BUN, 25.0 mg/dL; creatinine, 1.20 mg/dL; 24-hour CrCl, 91.0 mL/min/1.73 m^2; early morning urinary protein, 3+ (as measured by using a dipstick test); urinary protein to urinary creatinine ratio, 2.7 (milligram/milligram); daily urinary protein, 3.1 g; and urinary β-2 microglobulin, 0.064 mg/dL. At the latest follow-up (24 years of age), his renal function was stable (BUN: 25.0 mg/dL; creatinine: 1.20 mg/dL) with ACEI treatment, and he had not developed Wilms' tumor.

Patient 3

Patient 3 was a female with aniridia and mental retardation. G-banding revealed deletion of chromosome 11p13-p14 in one allele (Fig 2C), and she was therefore diagnosed with WAGR syndrome. The patient developed proteinuria at

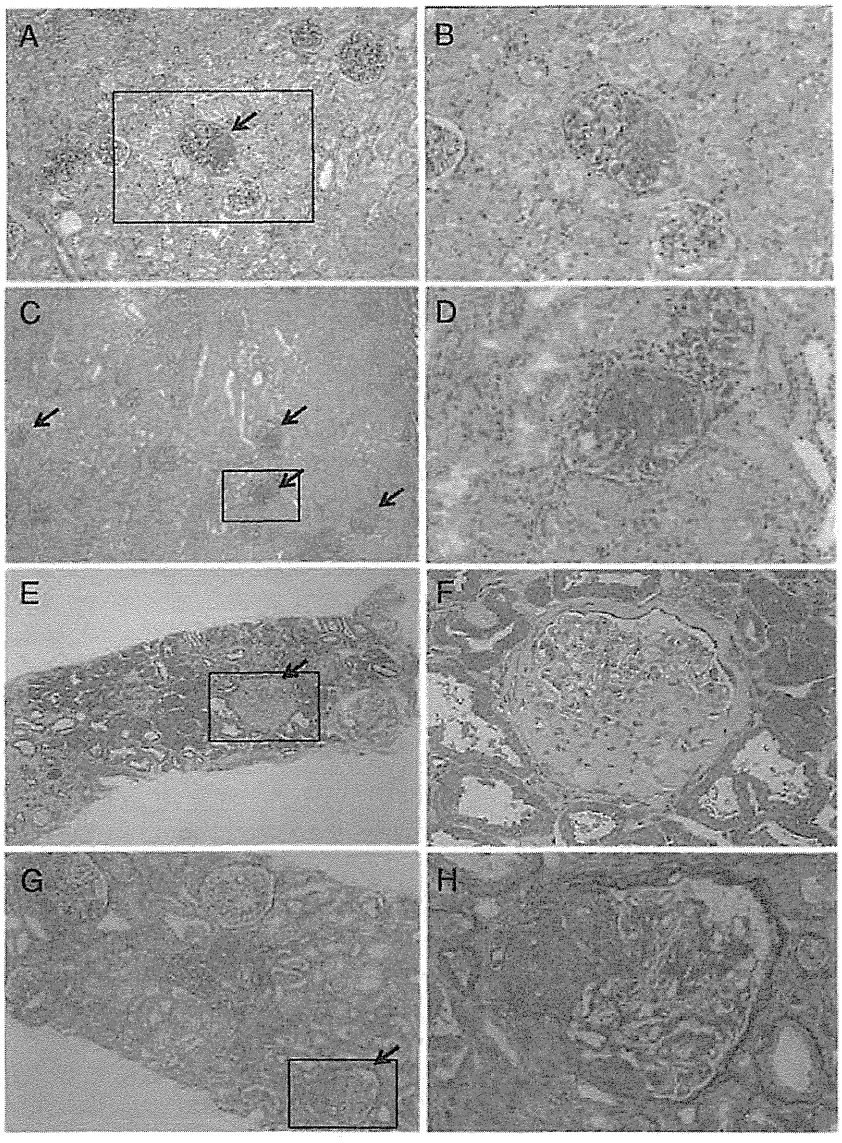

FIGURE 1

Renal histology. A, C, E, and G, Low magnification. B, D, F, and H, High magnification. Arrows show glomeruli with segmental glomerulosclerosis. A and B, Nephrectomized right kidney from patient 1. Patient 1 had no proteinuria at the time of nephrectomy. However, a few glomeruli exhibited segmental glomerulosclerosis although there were no immature glomeruli. C and D, Renal biopsy of left kidney from patient 1. Twenty-eight of 50 glomeruli showed segmental glomerulosclerosis. There were no tubulointerstitial lesions. E and F, Renal biopsy from patient 2. Two of eight glomeruli showed segmental glomerulosclerosis with interstitial fibrosis. G and H, Renal biopsy from patient 3. Ten of 30 glomeruli showed segmental glomerulosclerosis with interstitial fibrosis. All 3 patients exhibited FSGS (not otherwise specified).

the age of 6 years and nephrotic syndrome with normal renal function at age 15 years (urinary protein to urinary creatinine ratio, 10.6 [milligram/milligram]; total protein, 5.6 g/dL; albumin, 2.3 g/dL; BUN, 15.0 mg/dL; creatinine, 0.65 mg/dL; estimated glomerular filtration rate, 100.7 mL/min/1.73 m^2). We were unable to obtain her parents' consent for renal biopsy, and they chose to start drug treatment. However, treatment with prednisolone and ACEI was not effective, and her renal function gradually deteriorated. Therefore, she underwent renal biopsy at age 19 years. At the time of biopsy, her height was 144.5 cm, weight was 72.5 kg, and blood pressure was 130/83 mm Hg. Biochemical data were as follows: total protein, 5.5 g/dL; albumin, 2.5 g/dL; BUN, 30.0 mg/dL; creatinine, 1.40 mg/dL; 24-hour CrCl, 44.65 mL/min/1.73 m^2; early morning urinary protein, 3+ (as measured by using a dipstick test); daily urinary protein, 5.89 g; and urinary β-2 microglobulin, 0.495 mg/dL. Renal biopsy findings were consistent with FSGS (Fig 1 G and H). To date, she has not developed Wilms' tumor.

DISCUSSION

The current study demonstrated that 3 patients with atypical WAGR syndrome developed heavy proteinuria with FSGS, suggesting that the nephropathy seen in this syndrome is responsible for the FSGS lesion.

Patient 1 had possible bilateral Wilms' tumor and underwent unilateral nephrectomy, chemotherapy, and radiotherapy. Therefore, it is possible that the treatment of the remaining kidney for bilateral tumor or nephrogenic rest might account for the development of FSGS. However, the kidney nephrectomized after the first chemotherapy session but before radiotherapy treatment already showed segmental sclerosis in a few glomeruli, suggesting that radiotherapy was not the main cause of FSGS. Chemotherapeutic drugs such as adriamycin may induce FSGS as well as tubulointerstitial inflammation and fibrosis.[7] However, there were no tubulointerstitial lesions, suggesting that chemotherapy might not have been the main cause of FSGS. Nevertheless, it is possible that surgical renal ablation caused FSGS in patient 1.

Patients 2 and 3 did not develop Wilms' tumor during the course of clinical observation, and thus they did not undergo nephrectomy, chemotherapy, or radiotherapy, thereby eliminating any effect of these therapies on renal

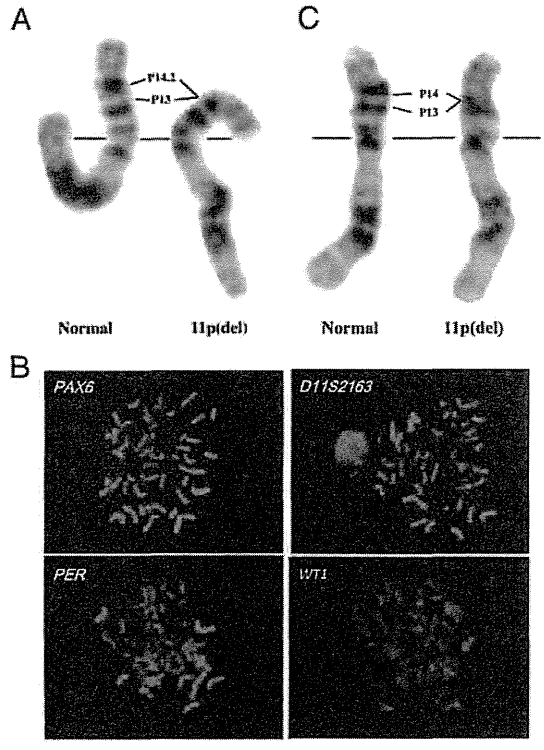

FIGURE 2

High-resolution G-banding of chromosome 11 and fluorescence in situ hybridization (FISH) in patient 2 and G-banding of chromosome 11 in patient 3. A, Patient 2 had deletion of chromosome 11p13-p14.2 in one allele. B, FISH using P1-derived artificial chromosome clones (1083G3 for *PAX6*; 65P5 for *D11S2163*; 685F3 for *PER*; and 104M13 for *WT1*) as probes was performed for patient 2, as previously reported.[6] Each FISH signal for *PAX6, D11S2163, PER, and WT1* was observed in only one chromosome 11 homolog, indicating heterozygous deletion of the WAGR region of 11p. C, Patient 3 had deletion of chromosome 11p13-p14 in one allele.

histology. The possibility of reflux nephropathy, however, could not be ruled out in patient 2. The perihilar variant with glomerular hypertrophy is particularly common in the secondary FSGS such as reduced renal mass–induced FSGS.[8] However, all 3 patients exhibited FSGS (not otherwise specified) without glomerular hypertrophy, suggesting that surgical renal ablation (patient 1) and reflux nephropathy (patient 2) may not have been the main cause of FSGS in these 2 patients. These findings suggest that the complete deletion of one *WT1* allele might have a pathogenetic role in the development of nephropathy.

The spectrum of glomerular diseases associated with *WT1* mutations has been reviewed.[9] *WT1* mutations can cause syndromic and nonsyndromic glomerular disease. The syndromic forms include DDS (early-onset nephrotic syndrome with diffuse mesangial sclerosis [DMS]); 46,XY disorders of sex development and Wilms' tumor; and Frasier syndrome (disorders of sex development, FSGS, and gonadoblastoma), which is caused by a mutation in the intron 9 splice site of *WT1* leading to the loss of the +KTS isoform of the protein. Mutations associated with both syndromic and nonsyndromic glomerular disease tend to cluster in exons 8 and 9 of *WT1*, which encode zinc fingers 2 and 3.[9,10] Orloff et al[11] reported that single-nucleotide polymorphisms in *WT1* may modulate the development of FSGS by altering *WT1* function. The current study suggests that complete deletion of one *WT1* allele may also induce the development of nephropathy.

Reduced expression levels of *Wt1*-induced glomerulopathies (crescentic glomerulonephritis or DMS) depending on gene dosage derived by combining *Wt1*-knockout mice and an inducible *Wt1* yeast artificial chromosome transgenic mouse model.[12] Eleven percent of mice heterozygous for the *Wt1* mutation showed severe proteinuria and DMS with tubular cysts, protein casts, and severe interstitial inflammation, although nephrogenesis was not delayed.[12] These findings indicate that the expression level of *WT1* plays an important role, not only during nephrogenesis but also in the homeostasis of normal kidney function. These findings also support our conclusion that complete deletion of one *WT1* allele in atypical WAGR syndrome could induce glomerulopathy without delayed nephrogenesis, although the reason for the discrepancy in histologic findings between man (FSGS) and mouse (DMS) is unclear.

CONCLUSIONS

Besides dominant-negative missense mutations in the eighth or ninth exon of *WT1* and mutations at the donor splice site of intron 9, complete deletion of one *WT1* allele may induce the development of FSGS. The findings in this study also suggest that haploinsufficiency of *WT1* could be responsible for the development of FSGS.

REFERENCES

1. Miller RW, Fraumeni JF Jr, Manning MD. Association of Wilms' tumor with aniridia, hemihypertrophy and other congenital malformations. *N Engl J Med*. 1964;270:922–927
2. Little MH, Williamson KA, Mannens M, et al. Evidence that WT1 mutations in Denys-

Drash syndrome patients may act in a dominant-negative fashion. *Hum Mol Genet.* 1993;2(3):259–264

3. Huff V. Genotype/phenotype correlations in Wilms' tumor. *Med Pediatr Oncol.* 1996;27 (5):408–414
4. Breslow NE, Takashima JR, Ritchey ML, Strong LC, Green DM. Renal failure in the Denys-Drash and Wilms' tumor-aniridia syndromes. *Cancer Res.* 2000;60(15):4030–4032
5. Kawase E, Tanaka K, Honna T, Azuma N. A case of atypical WAGR syndrome with anterior segment anomaly and microphthalmos. *Arch Ophthalmol.* 2001;119(12): 1855–1856
6. Muto R, Yamamori S, Ohashi H, Osawa M. Prediction by FISH analysis of the occurrence of Wilms tumor in aniridia patients. *Am J Med Genet.* 2002;108(4):285–289
7. Lee VW, Harris DC. Adriamycin nephropathy: a model of focal segmental glomerulosclerosis. *Nephrology (Carlton).* 2011;16 (1):30–38
8. D'Agati VD. The spectrum of focal segmental glomerulosclerosis: new insights. *Curr Opin Nephrol Hypertens.* 2008;17(3):271–281
9. Niaudet P, Gubler MC. WT1 and glomerular diseases. *Pediatr Nephrol.* 2006;21(11): 1653–1660
10. Mucha B, Ozaltin F, Hinkes BG, et al; Members of the APN Study Group. Mutations in the Wilms' tumor 1 gene cause isolated steroid resistant nephrotic syndrome and occur in exons 8 and 9. *Pediatr Res.* 2006; 59(2):325–331
11. Orloff MS, Iyengar SK, Winkler CA, et al. Variants in the Wilms' tumor gene are associated with focal segmental glomerulosclerosis in the African American population. *Physiol Genomics.* 2005;21(2): 212–221
12. Guo JK, Menke AL, Gubler MC, et al. WT1 is a key regulator of podocyte function: reduced expression levels cause crescentic glomerulonephritis and mesangial sclerosis. *Hum Mol Genet.* 2002;11(6): 651–659

Journal of Human Genetics (2012) 00, 1–8

www.nature.com/jhg

ORIGINAL ARTICLE

Subtelomeric deletions of 1q43q44 and severe brain impairment associated with delayed myelination

Keiko Shimojima[1], Nobuhiko Okamoto[2], Yume Suzuki[3], Mari Saito[3], Masato Mori[3], Tatanori Yamagata[3], Mariko Y Momoi[3], Hideji Hattori[4], Yoshiyuki Okano[4], Ken Hisata[5], Akihisa Okumura[5] and Toshiyuki Yamamoto[1]

Subtelomeric deletions of 1q44 cause mental retardation, developmental delay and brain anomalies, including abnormalities of the corpus callosum (ACC) and microcephaly in most patients. We report the cases of six patients with 1q44 deletions; two patients with interstitial deletions of 1q44; and four patients with terminal deletions of 1q. One of the patients showed an unbalanced translocation between chromosome 5. All the deletion regions overlapped with previously reported critical regions for ACC, microcephaly and seizures, indicating the recurrent nature of the core phenotypic features of 1q44 deletions. The four patients with terminal deletions of 1q exhibited severe volume loss in the brain as compared with patients who harbored interstitial deletions of 1q44. This indicated that telomeric regions have a role in severe volume loss of the brain. In addition, two patients with terminal deletions of 1q43, beyond the critical region for 1q44 deletion syndrome exhibited delayed myelination. As the deletion regions identified in these patients extended toward centromere, we conclude that the genes responsible for delayed myelination may be located in the neighboring region of 1q43.
Journal of Human Genetics advance online publication, 21 June 2012; doi:10.1038/jhg.2012.77

Keywords: 1q44 deletion; abnormalities of the corpus callosum; *AKT3*; delayed myelination; microcephaly; subtelomeric deletion; *ZNF238*

INTRODUCTION

Submicroscopic subtelomeric chromosomal deletions have been found in 7.4% of children with moderate to severe mental retardation.[1] Some subtelomeric deletion syndromes are clinically recognizable and identified by characteristic features, whereas some others cannot be identified by such means. The recent development of molecular karyotyping using chromosomal microarray testing has revealed clear genotype–phenotype correlations and identified the critical chromosomal regions of the characteristic features of subtelomeric deletions. The most striking example is the Miller-Diecker syndrome, which has shown clear genotype–phenotype correlations.[2] Miller-Diecker syndrome is caused by the subtelomeric deletion of 17p, and is well recognized and characterized by lissencephaly and distinctive facial features,[3] which result from the involvement of the platelet-activating factor acetylhydrolase 1b regulatory subunit 1 gene (*PAFAH1B1*) and tyrosine 3-monooxygenase/tryptophan 5-monooxygenase-activation protein epsilon polypeptide gene (*YWHAE*), respectively; both these genes are located on 17p13.[3]

Several studies have investigated the critical region for 1q44 subtelomeric deletion syndrome and found that the core phenotypic features of 1q44 subtelomeric deletion syndrome are microcephaly, abnormalities of the corpus callosum (ACC) and seizures.[4–16] Recently, Ballif *et al.*[17] analyzed patients with microdeletions of 1q44 and proposed certain genes that may be responsible for individual features.

We report the cases of six newly identified patients with 1q44 deletions; two with interstitial deletion of 1q44; and four with terminal deletion of 1q. As the patients with terminal deletion of 1q44 exhibited more severe phenotypes compared with the patients with interstitial deletion, the phenotypic differences would be derived from additionally deleted region of 1q43q44.

MATERIALS AND METHODS

Subjects

Six Japanese patients were diagnosed as having chromosomal deletions in the region of 1q43q44 in our ongoing study to analyze genomic copy number aberrations. This study was approved by the ethical committee of our institution. After obtaining written consents, we accumulated samples from the patients. Parental samples were also obtained to study their carrier status.

[1]Tokyo Women's Medical University Institute for Integrated Medical Sciences (TIIMS), Tokyo, Japan; [2]Department of Medical Genetics, Osaka Medical Center and Research Institute for Maternal and Child Health, Izumi, Japan; [3]Department of Pediatrics, Jichi Medical University, Shimotsuke, Japan; [4]Department of Pediatrics, Osaka City University School of Medicine, Osaka, Japan and [5]Department of Pediatrics, Juntendo University School of Medicine, Tokyo, Japan
Correspondence: Dr T Yamamoto, Tokyo Women's Medical University Institute for Integrated Medical Sciences (TIIMS), 8-1 Kawada-cho, Shinjuku-ward, Tokyo 162-8666, Japan.
E-mail: yamamoto.toshiyuki@twmu.ac.jp
Received 10 April 2012; revised 24 May 2012; accepted 25 May 2012

Methods

Genomic copy number was analyzed using the 244, 105 or 60 K Human Genome CGH Microarray (Agilent Technologies, Santa Clara, CA, USA) as described previously.[2] Genomic DNAs was extracted from peripheral blood using a standard method. Genomic copy number aberrations were visualized using Agilent Genomic Workbench version 5.5 (Agilent Technologies).

Fluorescence *in situ* hybridization (FISH) was performed as previously described, when metaphase spreads were available.[2] Bacterial artificial clones were selected from the UCSC genome browser (http://www.genome.ucsc.edu). Physical positions refer to the March 2009 human reference sequence. Bacterial artificial clone DNAs were extracted by an automatic DNA extraction system GENE PREP STAR PI-80X (Kurabo, Osaka, Japan).

RESULTS

Chromosomal deletions

Chromosomal microarray testing revealed aberrations in the 1q43q44 region in six patients (Figure 1). In patient 1 and 2, interstitial deletions of 1.9 and 2.2 Mb, respectively, were identified within the 1q43q44 region. In patient 1, FISH analysis confirmed the deletion (Figure 2a). Subsequent FISH analysis revealed no abnormalities in the parents of both families, indicating *de novo* deletions in both patients. Molecular karyotyping defined the aberrations as arr 1q44(243 809 193–245 665 521) × 1 dn for patient 1 and arr 1q43q44(243 303 991–245 506 920) × 1 dn for patient 2.

In patient 3, terminal deletions of 1q43 were identified and confirmed by FISH analyses (Figure 2b). As FISH analyses for both parents showed no abnormalities, this deletion occurred as *de novo*. Molecular karyotyping of patient 3 was indicated as arr 1q43q44(242 442 098–249 250 621) × 1 dn.

In patient 4, a loss of genomic copy number at 1q43q44 and an additional gain at 5p15.33 were identified (Supplementary Figure 1). Subsequent FISH analysis confirmed an unbalanced translocation between 1q43 and 5p in patient 4 (Figures 2c–e), and no translocation was found in either parents. Consequently, the patient's unbalance translocation was determined to be *de novo* in origin. Her karyotype was 46,XX,der(1)t(1;5)(q43;p15.33).arr 1q43q44(242 223 230–249 212 668) × 1, 5p15.33(57 640–1 705 515) × 3 dn. The duplicated region of 5p was only 1.7 Mb of the terminal region.

In patient 5, terminal deletions of 1q43 were identified with a breakpoint in the v-akt murine thymoma viral oncogene homolog 3 gene (*AKT3*). The molecular karyotype was arr 1q44(243 880 099–249 212 668) × 1. The largest deletion was identified in patient 6 with arr 1q43q44(238 888 870–249 212 668) × 1.

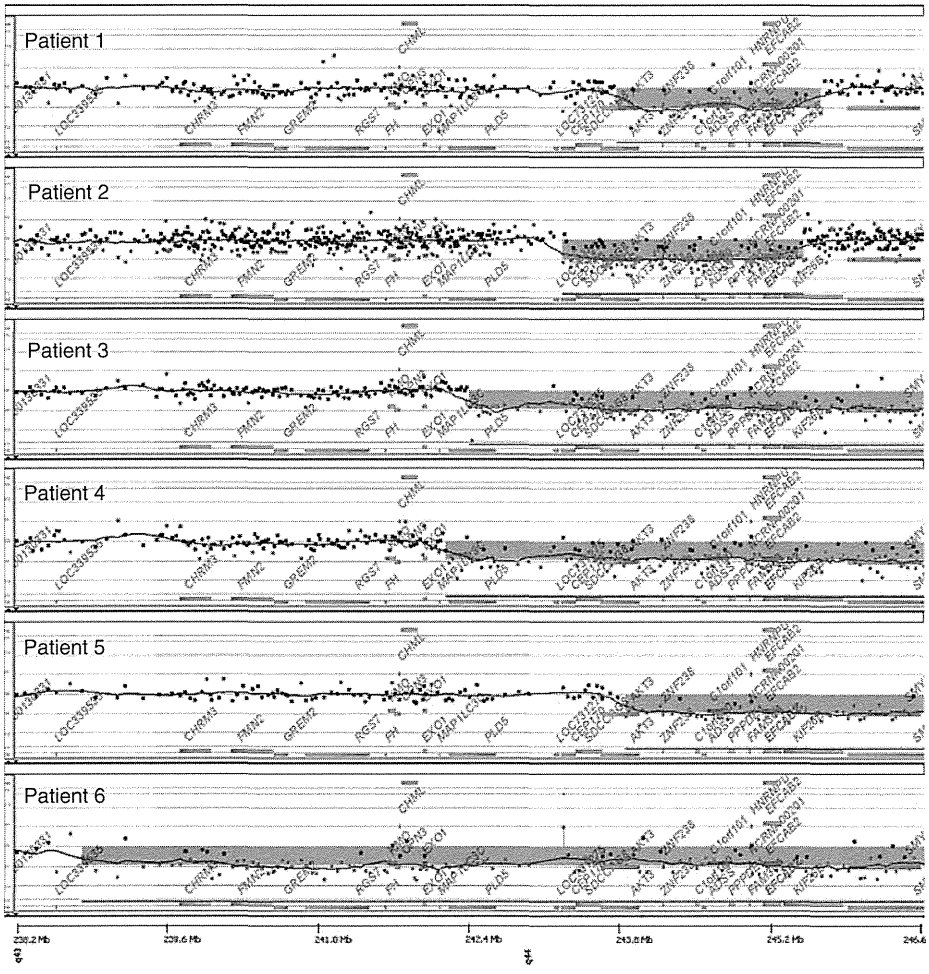

Figure 1 Results of chromosomal microarray testing presented by Gene View of Agilent Genomic Workbench (Agilent Technologies). Vertical axis and horizontal axis represent $\log_2$ signal ratio and genomic position, respectively. Aberrant regions are shown by blue rectangles. Dots indicate the genomic positions and the $\log_2$ ratio of each probe.